UNIVERSITÀ DEGLI STUDI DI PADOVA

DIPARTIMENTO DI FISICA E ASTRONOMIA
"GALILEO GALILEI"

CORSO DI LAUREA TRIENNALE IN ASTRONOMIA

Stellar winds in M-type AGB stars: the role of dust grains and pulsation

Venti stellari in stelle AGB di tipo M: ruolo dei grani di polvere e della pulsazione

Relatore Professoressa Paola Marigo
Co-relatore Dottoressa Sara Bladh

Laureando Alessandro Mazzi
n°1052041

A.A. 2015-2016

Contents

Abstract

It is a matter of fact that stars are subject to mass loss events which may be periodic, semi-periodic or episodic and can vary from insignificant to massive. A quantitative description of this phenomenon is necessary to assemble an accurate model for the evolution of stars and galaxies. Such description requires realistic dynamical models that follow the flow of stellar matter from the atmosphere through the wind acceleration zone into the circumstellar region. Three main aspects characterize the mass loss phenomenon in asymptotic giant branch stars: long-period pulsations with the production and propagation of shock-waves through the atmosphere; dust formation in the region where the temperature is low enough for the formation of grains; momentum transfer from the radiation field to the dust particles together with dust-gas and gas-gas collision.
In the first chapter I present a short review of the evolution of stars up to the AGB phase and the main events that are typical of that stage of evolution. In the second chapter the topic of dust driven stellar winds is introduced from a general point of view through the analysis of the fundamental mechanisms at the base of wind formation. Finally, in the third chapter I discuss the problem of driving a dusty wind in an M-type star. Oxides and pure silicates have low opacities in the relevant spectral region while dirty silicates, which should be good candidates due to their high opacity, can form only at large distances from the star. I also highlight a recently proposed solution that invokes scattering on large dust grains (with sizes of a few tenths of a micron) and an interesting argument based on the hypothesis that the process of chemisputtering may be negligible in the atmospheres of AGB stars.

Chapter 1

Asymptotic Giant Branch stars

A brief introduction of the Asymptotic Giant Branch (AGB) evolution following the thorough review by Habing and Olofsson (2004) is presented in the next sections.

1.1 Pre-AGB evolution of low- and intermediate-mass stars

Starting from the zero-age main sequence, the star burns H in the core until it is exhausted. The star then leaves the main sequence and the helium core contracts.
If the mass of the star lays between $0.9M_{\odot}$ and $1.8-2.0M_{\odot}$ the helium core becomes degenerate and H is ignited in a shell. This burning shell causes the expansion of the star and the formation of a convective zone in the outer layers. When the star approaches the Hayashi line the convective envelope grows inwards in mass and reaches the region where the partial H burning occurred (first dredge up) enriching the surface with ^{4}He, ^{14}N and ^{13}C. As the star ascends the giant branch, the He core continues to contract and heat until the triple-alpha reactions are ignited off-center, due to neutrino losses, in a highly degenerate condition, causing the helium core flash. The increase of the temperature eventually lifts the degeneracy of the core and the star quiescently burns He in a convective core also burning H in a shell. Figure 1.1 shows the evolution of a low-mass star on the HR diagram.
On the other hand, if the star has a mass between $2M_{\odot}$ and $6-8M_{\odot}$, the ignition of He occurs in the core under non degenerate conditions, surrounded by the H-burning shell. During the He-burning phase the star may experience a blue loop on the HR diagram.
The subsequent phase of evolution is common to both low- and intermediate-mass stars.

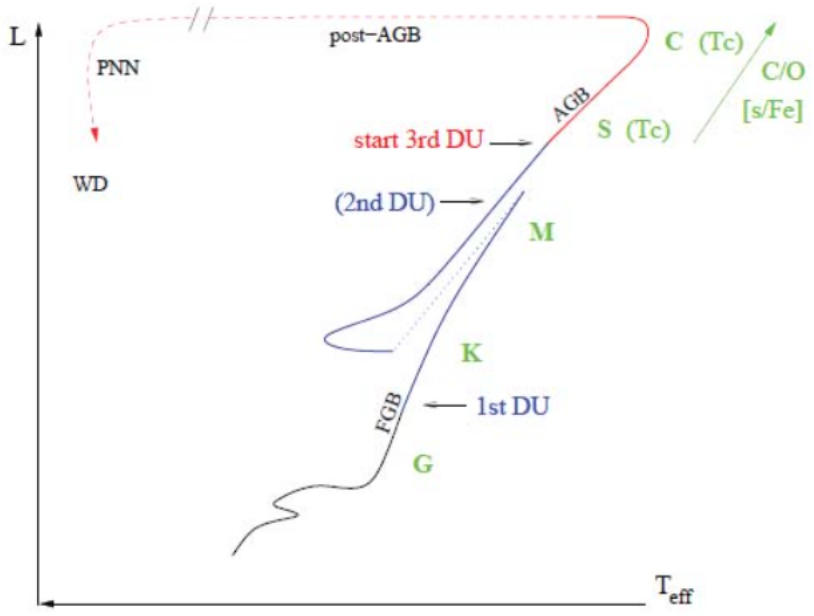

Figure 1.1: Evolution on the HR diagram of a low-mass star with the occurrence of dredge-up events.

1.2 AGB evolution and structure

Following the exhaustion of helium in the core, the star approaches for the second time the Hayashi line and evolves along the so-called Asymptotic Giant Branch. It is common practice to distinguish two phases: the Early-AGB phase and the Thermal Pulsing AGB phase.

1.2.1 Early AGB evolution

At the beginning of the early AGB phase the star develops a He-burning shell around the inert C-O core while maintaining the H burning shell and a double mirror-effect takes place. The core contracts, the He-rich layers above expand and the outer envelope starts contracting. Due to the expansion of the He-rich zone, the H-burning shell cools down until it extinguishes. The entire envelope then expands in response to core contraction. The He-burning shell gradually adds mass to the C-O core, leading to degeneracy. The convective envelope cools down due to the expansion and moves inward until it reaches the composition discontinuity left by the extinguished H shell (point K in figure 1.2). For stars whose mass is larger than $4M_{\odot}$ the second dredge-up may occur. The convective envelope penetrates enough to reach the He-rich layers. In low-mass stars however the H-burning shell remains active at a low level, preventing the second dredge-up. In the dredged up material we find

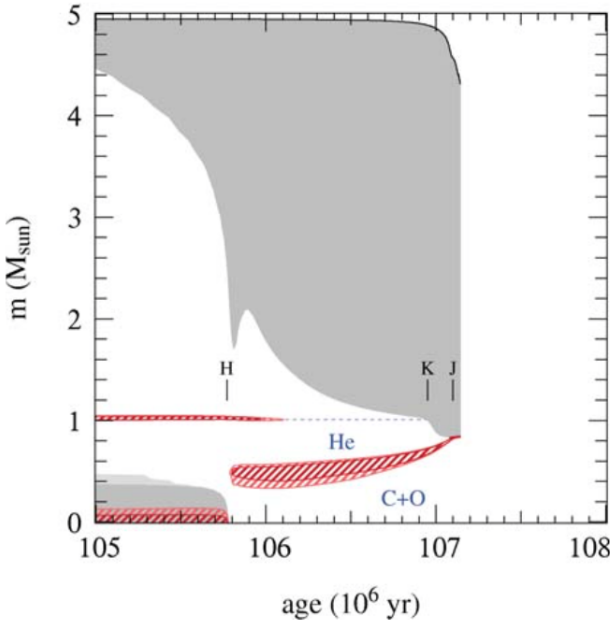

Figure 1.2: Evolution of the internal structure of a $5M_{\odot}$ star with time. The early AGB starts at point H. The H-burning shell extinguishes and at point K the second dredge-up occurs. The H-burning shell re-ignites at point J.

helium, obtained from H burning, and ^{14}N, obtained through the CNO cycle, which are mixed into the convective envelope and appear at the surface.

1.2.2 Thermal pulsing AGB evolution

As the He-burning shell approaches the H-He discontinuity it decreases its luminosity due to the lack of fuel. The layers above contract until the H-burning shell is re-ignited. The He-burning shell becomes thin and the on-going nuclear burning become thermally unstable thus this shell undergoes periodic thermal pulses, giving the name to this phase: thermally pulsating AGB.
While the He shell is inactive, the H-burning shell adds mass to the He-rich intershell, increasing its pressure on the underlying shell. When the mass of the intershell reaches a critical value He is ignited in an unstable manner giving rise to a thermonuclear runaway (helium shell flash). The large energy flux drives convection in the whole intershell region, which mixes products of the 3-α reaction (^{12}C), but also drives the expansion of the intershell and eventually of the He-shell itself, quenching the flash due to cooling. The expansion also determines the extinguishing of the H-burning shell. He is then burned quiescently in the shell for a hundred years. Another effect of the expansion and cooling is that the outer convective envelope penetrates

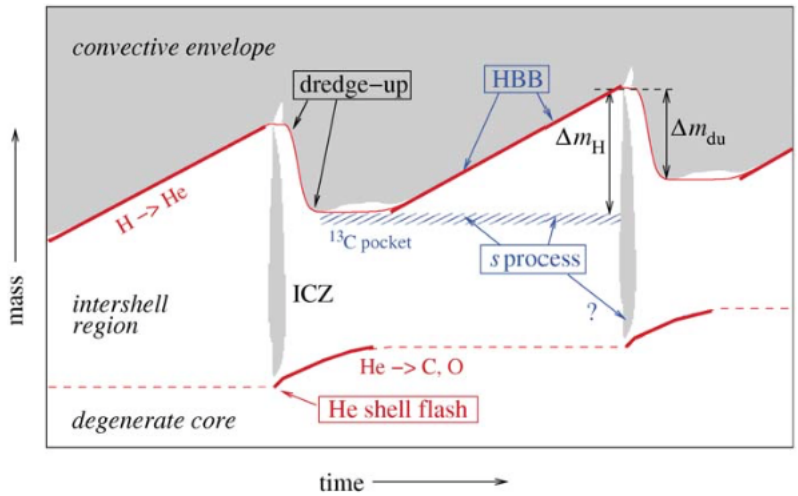

Figure 1.3: Evolution of an AGB star through two thermal pulse cycles. Convective regions are grey. Thick lines indicate active burning while thin lines (both solid and dashed) stands for inactive shells. The time interval is non-linear since the interpulse phase lasts $10^4 - 10^5$ years while the He-shell flash and dredge-up episodes lasts ~ 100 years.

deeper into the star, in some cases even beyond the now extinct H-burning shell, mixing material form the intershell into the outer envelope. This event is called third dredge-up, even for stars that do not experience the second dredge-up, and brings to the surface He and products of He-burning. After the third dredge-up the H-shell re-ignites while the He-shell shuts down. A long phase of stable H-burning follows, during which the mass of the intershell increases until the next thermal pulse occurs. Figure 1.3 shows two consecutive thermal pulse and the relative dredge-up events.

1.2.3 Nucleosynthesis

At the beginning of the AGB phase the star has a dense, small, degenerate core made of ^{12}C and ^{16}O. On top of the degenerate core lies the He-burning shell and after a thin intershell region there is the H-burning shell. The second dredge-up then brings to the surface the products of H-burning, mostly occurred through the CNO cycle. As the H-shell advances in the envelope it burns H into ^{4}He and essentially all the CNO elements end as ^{14}N. This way, the abundances of ^{13}C, ^{14}N increase while the abundances of ^{12}C, ^{16}O and ^{18}O decrease. The He-burning shell processes the ^{14}N into ^{22}Ne through the capture of two α-particles and produces ^{12}C with triple-alpha reactions. Also ^{23}Na and ^{25}Mg as well as s-process elements are produced.
As outlined in section 1.2.2, during a thermal pulse the convective zone

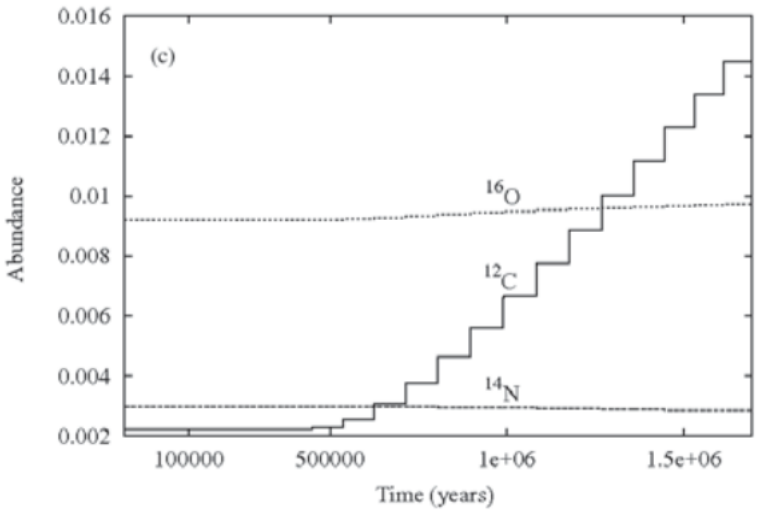

Figure 1.4: Variation of the abundance of ^{12}C and ^{16}O as well as ^{14}N during the TP-AGB phase of a $3M_{\odot}$ star due to the third dredge-up.

deeply penetrates into the star and reaches the layers where the nuclear processes took place, bringing new materials upwards thus changing the composition of the surface of the star, enriching it especially with ^{12}C. If this process goes on for a sufficient amount of time the C/O ratio may become higher than one and the star becomes a carbon star, as shows figure 1.4.
However if the mass of the star is large enough ($\sim 4 - 5M_{\odot}$), the base of the convective envelope may become hot enough ($T > 3 \times 10^7$ K) to activate the CNO cycle in a process known as *hot bottom burning*. As a consequence, carbon will be burned into nitrogen before reaching the stellar surface in a process known as hot bottom burning that prevents the formation of a carbon star. The hot bottom burning also produces ^{7}Li, ^{23}Na, ^{25}Mg and ^{26}Mg.
In addition to the effects of nuclear reactions and dredge-ups, the surface chemistry reflects the abundances of the elements of the star and is controlled by the C/O ratio. In fact, the chemistry will be dominated by the most abundant element between C and O, while the other will be locked in the CO molecule due to its stability.

1.2.4 Atmosphere

The outer part of the star is cool enough to allow the formation of molecules that ultimately determine the appearance of the spectrum of the star at least in the near-IR, also influencing the structure of the atmosphere itself. The pulsation of the star levitates the weakly bound external layers, giving the atmosphere a larger scale height. At large distances from the star, grain condensation takes place and particles may leave the star if their velocity is higher than the escape velocity, resulting in the formation of a stellar wind.

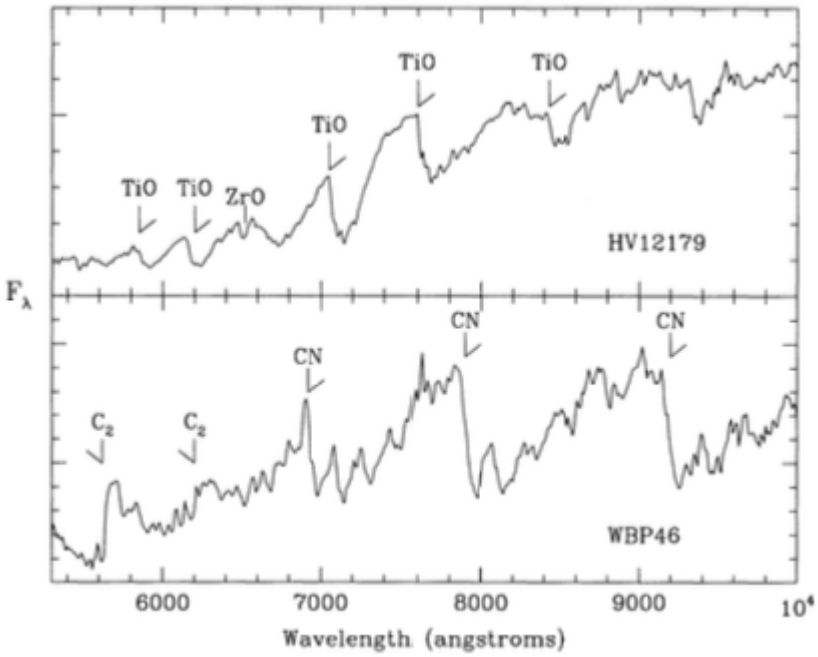

Figure 1.5: Spectra of an M star and a C star with indication of the strongest molecular bands. From Habing and Olofsson (2004).

AGB stars are divided in three groups based on their spectra: M-type stars have strong TiO bands so they should have C/O<1; C-type stars have strong molecular bands from carbon compounds and metallic oxides are absent, thus should have C/O>1; lastly S-type stars should have approximately C/O=1 and are characterized by ZrO bands. Figure 1.5 shows the spectra of an M-type star and a C-type star and their respective characterizing bands. More details on the effects of the C/O ratio are given in chapter 2.
Another observable characteristic of AGB stars is the long-period variation of their flux which is a direct consequence of the pulsation of their atmosphere. There are four different categories of AGB stars, based on the appearance of their light curve: Mira-like ("M") stars have regular variations with a large amplitude in the V-band ($\Delta V \geq 2.5$) and periods >20 days up to 2000 days; semi-regular of type a ("SRa") which are relatively regular with a smaller amplitude in the V-band ($\Delta V < 2.5$); semi-regular of type b ("SRb") which feature poor regularity with a small amplitude in the V-band ($\Delta V < 2.5$); Irregular ("L") with irregular variations of low amplitude. Some stars, however, do not fit exactly into just one of the categories.

1.2.5 Stellar winds and mass loss

The mass-loss process in AGB stars is fundamental for their evolution and for the enrichment of the interstellar medium and is tightly connected to the topic of the stellar wind.
Strong stellar winds from AGB stars are evident from a large excess at infrared wavelengths in their spectral energy distribution. In the simple picture, as AGB stars are found to undergo strong radial pulsations, shocks pass through the atmosphere bringing the gas to a larger radii and increasing the density. At $1.5 - 2.0 R_\star$, where the temperature is lower, dust particles form and are accelerated by the radiation pressure. The gas is then dragged along by the accelerated dust particles resulting in a large-scale outflow.
Observationally, there is a correlation between the pulsation period and the mass-loss rate. As a star evolves towards larger radii along the AGB, the pulsation period increases and so does the mass-loss rate.
As an AGB star loses mass in a slow (terminal velocities of $\sim 5 - 20$ km s^{-1}) but massive (from $10^{-8} M_\odot/yr$ to $10^{-4} M_\odot/yr$) outflow, a circumstellar envelope of escaping gas and dust particles forms around the star. Many AGB stars, known as OH/IR stars, are completely enshrouded in the dusty circumstellar envelope and are invisible at optical wavelengths. The gas is almost completely molecular and dominated by H_2. The molecules are located in shells of different radii depending on their bond energy and their formation paths. The dust is found only at larger radii (1.5-4R$_\star$). The composition of molecules and grains depends ultimately on the C/O ratio. At some point the circumstellar envelope merges into the interstellar medium, defining the outer limit of an AGB star. More details are given in Chapter 2 and Chapter 3.

Chapter 2

Dust driven stellar winds

Dusty stellar winds are typical of stars whose atmospheres are cool enough to allow the condensation and growth of dust grains. Generally, such winds have low velocities but are quite massive. AGB stars in particular have low effective temperatures but high luminosities, hinting that the wind may be driven by momentum transfer from the radiation field to the grains capable of condensing close enough to the star. However, the relatively low temperatures of the atmospheres of AGB stars are still high when compared to the condensation temperatures of most of the compounds that may form. This problem requires detailed modelling to be solved. The following dissertations are based on Lamers and Cassinelli (1999).

2.1 Stationary wind theory

Assuming an isothermal stellar wind in which the gas is subject only to the inward directed gravity and the outward directed gradient of the gas pressure, for a time-independent wind with a constant mass loss rate the equation of mass conservation holds:

$$\dot{M} = 4\pi r^2 \rho(r) v(r) \tag{2.1}$$

and the motion of the gas is described by the Newton's law $f = pdv/dt$. The velocity and location of a unit of mass accelerated in the wind in general depends on time and distance r so that

$$\frac{dv(r,t)}{dt} = \frac{\partial v(r,t)}{\partial t} + \frac{\partial v(r,t)}{\partial r}\frac{dr(t)}{dt} = v(r)\frac{dv}{dt} \tag{2.2}$$

but in a stationary hence time-independent wind $\partial v(r,t)/dt = 0$. If there are no other forces acting on the wind other than gravity and pressure, the equation of motion, called moment equation, is

$$v\frac{dv}{dr} + \frac{1}{\rho}\frac{dp}{dr} + \frac{GM_\star}{r^2} = 0 \tag{2.3}$$

If the flow behaves like a perfect gas $p = \mathcal{R}T\rho/\mu$ with $\mathcal{R}$ the gas constant and μ the mean atomic weight. The force due to the pressure gradient can be written as

$$\frac{1}{\rho}\frac{dp}{dr} = \frac{\mathcal{R}}{\mu}\frac{dT}{dr} + \frac{\mathcal{R}T}{\rho\mu}\frac{d\rho}{dr} = \left(\frac{\mathcal{R}T}{\mu}\right)\frac{d\rho}{dr} \tag{2.4}$$

where the second equality holds for an isothermal wind. The density gradient in turn can be written as

$$\frac{1}{\rho}\frac{d\rho}{dr} = -\frac{1}{v}\frac{dv}{dr} - \frac{2}{r}. \tag{2.5}$$

Using 2.4 and 2.5 in 2.3 gives, after some algebra,

$$\frac{1}{v}\frac{dv}{dr} = \left\{\frac{2a^2}{r} - \frac{GM_\star}{r^2}\right\} / \left\{v^2 - a^2\right\} \tag{2.6}$$

where $a = (\mathcal{R}T/\mu)^{1/2}$ is the isothermal speed of sound, constant in an isothermal wind. The lower boundary of equation 2.6 is the bottom of the isothermal region, r_0, in general near the photospheric radius.
The numerator of the moment equation 2.6 goes to zero at a distance

$$r_c = \frac{GM_\star}{2a^2} \tag{2.7}$$

called *critical distance* that defines the position of the *critical point*. It must be $r_c > r_0$ otherwise the critical point would be place din the underlying photosphere and the assumption of isothermal wind would not be valid. It is to be noted that dv/dr at r_c is equal to zero.
The condition $v = a$ instead nullifies the denominator but leads to an infinite velocity gradient. The only solution is that this should happens for $r = r_c$ thus nullifying both the numerator and the denominator. This is the *critical solution*, which is characterized by

$$v(r_c) = a \leftrightarrow r_c = \frac{GM_\star}{2a^2} \tag{2.8}$$

or similarly

$$v(r_c) = a = \frac{v_{esc}(r_c)}{2} \tag{2.9}$$

where $v_{esc} = 2GM_\star/rc$ is the escape velocity at the critical point. The point defined by $v(r) = a$ is called *sonic point*.
The critical solution is transonic: it starts subsonic at small distances and reaches supersonic velocities at larger distances.
While it is obvious that the case of a stationary wind is not fit to describe an AGB star, from the above discussion it is clear that a stellar wind requires a driving mechanism to accelerate the flow. In the case of cool stars such mechanism is generally represented by momentum transfer from the stellar radiation field to dust grains through absorption or scattering of light and from these to the gas particles through collisions.

2.2 Two step mechanism

The formation of winds in AGB stars is generally considered as the result of two processes: the pulsation of the star and the consecutive production of dust. The former provides denser and cooler layers where the latter can occur and finally drive the wind through the drag force. In the following sections i will briefly discuss these topics. I will leave the actual discussion on the formation and growth of dust grains to sections 2.3 and 2.4.

2.2.1 Role of dust

According to Bladh and Höfner (2012), it can be assumed that the condensates are subjected to just two opposite forces, the gravity and the radiation pressure, and the resulting acceleration may be written as

$$\frac{dv}{dt} = -a_{grav} + a_{rad} = -a_{grav}(1 - \Gamma) \tag{2.10}$$

Using the expression for the gravitational acceleration as a function of stellar parameters

$$\frac{dv}{dt} = -g_\star \left(\frac{R_\star}{r}\right)^2 (1 - \Gamma) \tag{2.11}$$

where v is the radial velocity of the fluid element at distance r from the center of the star and $g_\star = G\frac{M_\star}{R_\star^2}$.
The Γ is crucial for the generation of the wind and it can be expressed as

$$\Gamma = \frac{a_{rad}}{a_{grav}} = \frac{\langle k \rangle_H L_\star}{4\pi c G M_\star} \tag{2.12}$$

with $\langle k \rangle_H$ the flux-averaged dust opacity.
It is clear that the value of $\Gamma = 1$ defines a critical value for the dust opacity

$$k_{crit} = \frac{4\pi c G M_\star}{L_\star} \tag{2.13}$$

that implies $\frac{dv}{dt} = 0$. If $\Gamma < 1$ it means that the element will fall back following a ballistic trajectory after reaching a maximum distance from the star given by

$$\frac{R_\star}{r_{max}} = 1 - \left(\frac{v_0}{v_{esc}}\right)$$

where $v_{esc} = \sqrt{\frac{2GM_\star}{R_\star}}$ is the escape velocity from the surface of the star.
The condition $\Gamma > 1$ then means that the gust particle will be accelerated outwards and is the fundamental requirement to drive a dusty wind.
The expression for Γ shows different contributions to the acceleration of the element: the properties of the star, mass and luminosity, and the properties

of the element, meaning its material. Assuming that all the grains have equal radii, the collective opacity per mass of stellar matter is

$$k_{acc}(\lambda, a_{gr}) = \frac{\pi}{\rho} a_{gr}^2 Q_{acc}(\lambda, a_{gr}) n_{gr} \tag{2.14}$$

where n_{gr} is the number density of grains and Q_{acc} is the efficiency defined as the ratio between the radiative and the geometrical cross-section of an individual grain which can also be expressed as

$$Q_{acc} = Q_{abs} + (1 - g_{sca}) Q_{sca} \tag{2.15}$$

where g_{sca} is the asymmetry factor, describing deviations from isotropic scattering. In the small particle limit (grain radius $<<$ λ) $Q_abs \propto a_{gr}$ and $Q_{sca} \propto a_{gr}^4$.
Introducing the atomic weight of the monomer A_{mon}, the bulk density of the grain material ρ_{gr}, the abundance of the limiting element, which is the first element consumed, ϵ_{lim} and the degree of condensation of the limiting element f_c it can be written that

$$k_{acc}(\lambda, a_{gr}) = \frac{3}{4} \frac{A_{mon}}{\rho_{gr}} \frac{Q_{acc}(\lambda, a_{gr})}{a_{gr}} \frac{\epsilon_{lim}}{s(1 + 4\epsilon_{He})} f_c \tag{2.16}$$

where s is the stoichiometric coefficient.
In the small particle limit ($\lambda \gg 2\pi a_{gr}$) absorption dominates over scattering which means that $Q_{acc} \sim Q_{abs}$ and defining $Q'_{acc} = \frac{Q_{abs}}{a_{gr}}$ the opacity can be written as

$$k_{acc}(\lambda, a_{gr}) = \frac{3}{4} \frac{A_{mon}}{\rho_{gr}} Q'_{acc}(\lambda) \frac{\epsilon_{lim}}{s(1 + 4\epsilon_{He})} f_c \tag{2.17}$$

valid in the first stages of grain formation or until the particle is small compared to the wavelength. Figure 2.1 gives the trend of the efficiency per grain radius for different dust species.
Finally, the flux-averaged dust opacity can be calculated from the monochromatic grain opacity $k_{acc}(\lambda)$ and the monochromatic flux F_λ

$$\langle k \rangle_H = \frac{\int_0^\infty k_{acc}(\lambda) F_\lambda d\lambda}{\int_0^\infty F_\lambda d\lambda} \tag{2.18}$$

It is immediate that to drive a wind Q'_{acc} must be large in the wavelength region of the stellar flux maximum; nonetheless, f_c will be zero until dust grains start to condense but this can happen only in a relatively cool gas and if the grains are thermally stable. Grains temperature ultimately depend on their optical properties as well as on the stellar flux distribution and the distance from the star.
The condensates finally drive the wind through coupling with the gas particles. As the grains gain momentum from the stellar radiation filed they will collide on gas molecules and produce a drag force on them. This phenomenon also sets a lower limit on mass loss rate of about $10^{-7} M_\odot / yr$.

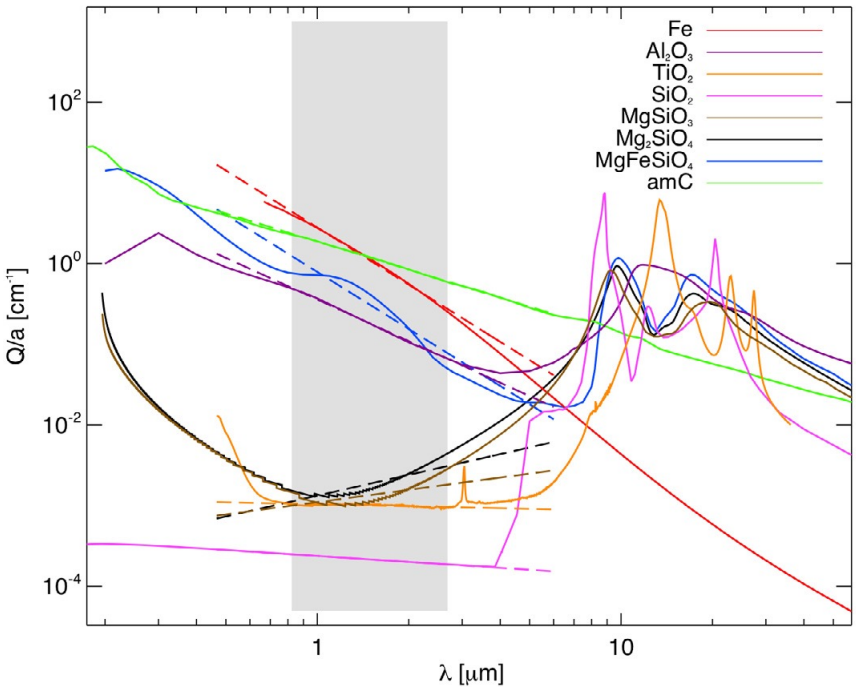

Figure 2.1: Efficiency per grain radius in the small particle limit as a function of wavelength for different dust species. The dashed lines show the power law fit. From Bladh and Höfner (2012).

2.2.2 Role of pulsation

The density of the gas is crucial to the formation of dust and to the drag force. In a static atmosphere it decreases with increasing distance form the star and it will be low at the typical distance at which the dust forms. As a consequence, the grains will have few collisions with the gas particles, resulting in no wind generation.

However, as outlined in the previous chapter, an AGB star pulsates, which means that its atmosphere is periodically pushed to a larger radius by the shock waves. This has two essential consequences: there will be temporary density-enhanced layers due to the shocks passing through the atmosphere and these layers will cool as they get further from the star. This situation of higher density and lower temperature allows the formation of some condensates, which are essential to driving a wind in cool stars, and allows the drag force to be large enough to drive an outflow.

Figure 2.2 shows the effects of the pulsation on a mass layer. The left panel shows a simple toy model: if the layer is pushed by pulsation at the condensation distance or even beyond, dust grains will form and drive an outflow. The right panel shows a more detailed model where the degree of condensation is indicated: without dust the layer will fall back onto the star however

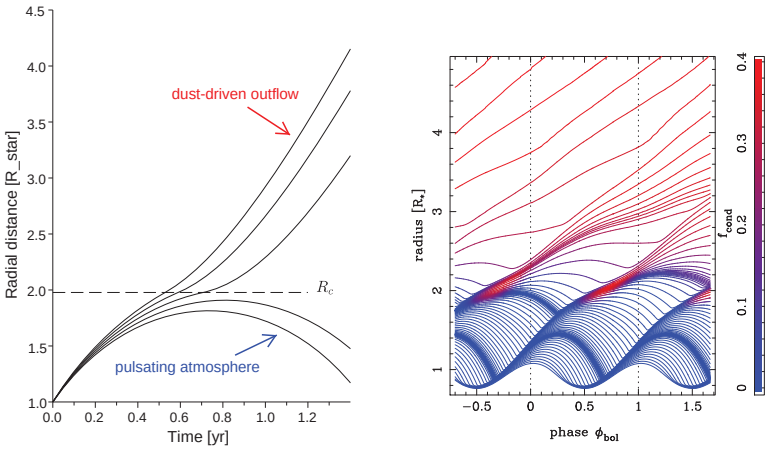

Figure 2.2: Dynamics of a shock levitated atmosphere and wind acceleration region in the pulsation-enhanced dust-driven scenario illustrated by tracking the motions of mass layers. Left panel: simple toy model (Höfner 2009). Right panel: a detailed radiation-hydrodynamical model (Nowotny et al. 2010) with indicated the degree of condensation. Both panels have similar stellar parameters. From Höfner (2015).

if enough dust forms it will move outwards.

2.3 Dust formation

To determine if a specific grain material can condense in the layers where the passing shock created conditions of higher density we need to introduce two variables: the levitation distance R_l, defined as the distance to which the pulsation induced shock levitates the gas in the atmosphere without radiative acceleration on the grains, and the condensation distance R_c, defined as the closest distance to the star where grains of a certain kind can exist. The following dissertation is based on Bladh and Höfner (2012).

2.3.1 Levitation distance

A simple estimate can be made ignoring heat loss and pressure effects so that there is complete conversion of the pulsation-induced kinetic energy into potential energy. If the gas has an initial velocity u_0 at distance R_0 then it is possible to write

$$\frac{mu_0^2}{2} - \frac{mM_\star G}{R_0} = -\frac{mM_\star G}{R_l}$$

and consequently

$$\frac{R_l}{R_\star} = \frac{R_0}{R_\star}\left[1 - \frac{R_0}{R_\star}\left(\frac{v_0}{v_{esc}}\right)^2\right]^{-1} \tag{2.19}$$

where

$$v_{esc} = \left(\frac{2M_\star G}{R_\star}\right)^{\frac{1}{2}}$$

Assuming as typical parameters of an AGB star $M_\star = 1M_\odot$, $L_\star = 5000L_\odot$ and $T_{eff} = 2800K$ the escape velocity at the surface is about $36km/s$. Radial velocities of the gas after a shock can be derived from observation of the second overtone CO line ($\Delta\nu = 3$) and are around $10 - 15km/s$. According to theoretical models these lines are originated from a region about 1.5 stellar radii above the stellar surface. If the gas initial velocity is of about 15 km s^{-1} at a distance of $1.5R_\star$ then $R_l \sim 2R_\star$. This is in agreement with the interferometric measurements that place at this distance the inner edge of dust shells around AGB stars.

2.3.2 Condensation distance

In a strong radiation field it is possible to assume that the temperature of the grains are determined by the condition of radiative equilibrium

$$k_{abs,J}J - k_{abs,S}S(T_d) = 0 \tag{2.20}$$

with J mean intensity and S source function, both integrated over the wavelength; k_{abs} is the dust absorption coefficient weighted either with J or S. If the atmosphere is optically thin, J_λ can be approximated by a geometrically diluted Planck distribution

$$J_\lambda = W(r)B_\lambda(T_\star) \tag{2.21}$$

where $T_\star$ is the effective temperature of the star and

$$W(r) = \frac{1}{2}\left[1 - \sqrt{1 - \left(\frac{R_\star}{r}\right)^2}\right]$$

is the geometric dilution factor, and it can be assumed that $S(T_d)$ is given by $B(T_d) = \int B_\lambda(T_d)d\lambda = \frac{\sigma}{\pi}T_d^4$.
With the given approximation the equation of radiative equilibrium can be reformulated as

$$k_{abs,B}(T_\star)W(r)T_\star^4 = k_{abs,B}(T_d)T_d^4 \tag{2.22}$$

Assuming $r \gg R_\star$ then $W(r) = \left(\frac{R_\star}{2r}\right)^2$ and

$$T_d \approx T_\star\left(\frac{R_\star}{2r}\right)^2\left(\frac{k_{abs,B}(T_\star)}{k_{abs,B}(T_d)}\right)^4 \tag{2.23}$$

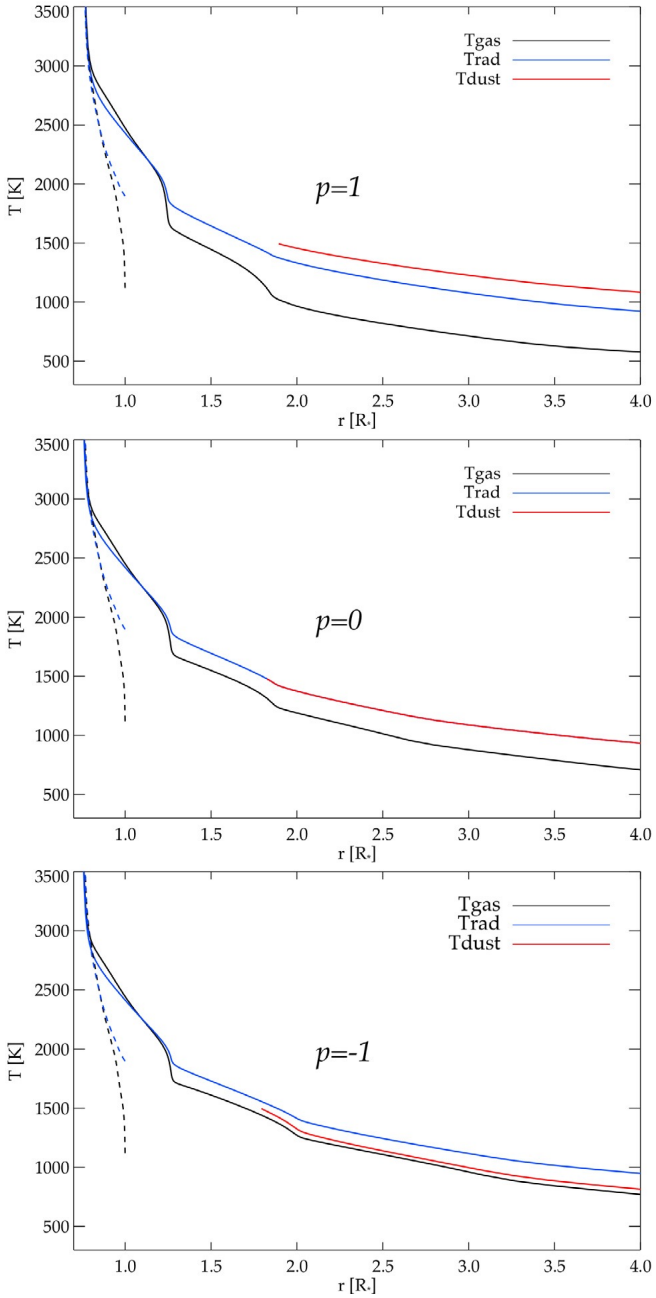

Figure 2.3: Effect on dust temperature of the power law coefficient p in a simple parametrized model. From Bladh and Höfner (2012).

If the absorption coefficient can be approximated by a power law in the relevant wavelength region then $k_{abs} \sim \lambda^{-p}$ and it is possible to use the simplification

$$\frac{k_{abs,B}(T_\star)}{k_{abs,B}(T_d)} = \frac{T_\star^p}{T_d^p} \tag{2.24}$$

resulting in

$$T_d \approx T_\star \left(\frac{R_\star}{2r}\right)^{-\frac{2}{4+p}} \tag{2.25}$$

Introducing the condensation temperature T_c and setting $T_d = T_c$ it is possible to solve for the condensation distance

$$\frac{R_c}{R_\star} = \frac{1}{2}\left(\frac{T_c}{T_\star}\right)^{-\frac{4+p}{2}} \tag{2.26}$$

The effect of the power law coefficient on the temperature of the dust is shown in figure 2.3 for three values of p.

2.4 Dust growth

Following Nanni et al. (2013), dust formation can be considered as a two-step process. First of all small stable refractory aggregates are formed from the molecules in the gas phase, called seed nuclei, then, with the decrease of temperature, accretion on their surface occurs by addition of more molecules.

2.4.1 Seed nuclei

Assuming that the grain size distribution of a certain dust species follows a power law such as

$$\frac{d\epsilon_i}{da_i} = A_i a^{-x_g} \tag{2.27}$$

where the size a is normalized to 1μm, A_i is the normalization constant and x_g is the same for every dust species, it is possible to determine a rough estimate of ϵ_i with the assumption that the number of seeds is equal to the number of grains needed to reproduce the observed local ISM extinction and

$$\epsilon_i = \int_{a_{min}}^{a_{max}} \frac{d\epsilon}{da_i} da \tag{2.28}$$

Assuming instead that the seeds correspond only to the fully grown grains with typical sizes a and mass $m_g = \frac{4}{3}\pi a^3 \rho_d$ it is possible to estimate their number from the grains needed to reproduce the total dust mass $M_i = \frac{\epsilon_{k,i}}{n_{k,i}} m_{d,i} N_H$ so that

$$\epsilon_i = \frac{M_i}{m_g}\frac{1}{N_H} \tag{2.29}$$

In the case of silicates, at varying metallicity it is logical to expect that the number of seeds will depend also on the abundance of the molecules that form the initial aggregates. It is possible to assume that in M-type stars the number of seeds has a dependence on metallicity like

$$\epsilon_{s,M} = \epsilon_s \left(\frac{Z}{Z_{ISM}} \right) \tag{2.30}$$

where $Z_{ISM} = 0.017$. For carbon stars an equation with the same meaning considers the dependence of the number of seeds on the abundance of carbon not locked in the CO molecule $\epsilon_{(C-O)} = \epsilon_C - \epsilon_O$ so that

$$\epsilon_{s,C} = \epsilon_s \left[\frac{\epsilon_{(C-O)}}{\epsilon_{(C-O),ISM}} \right] \tag{2.31}$$

2.4.2 Accretion of dust grains

The growth rate of a certain dust species is determined by the concurrent progress of two processes: collisions of molecules on the grain surface, and decomposition of the grain. The rate of the former is expressed by J_i^{gr}, the rate of the latter by J_i^{dec} and the differential equation describing dust growth is usually

$$\frac{dV_I}{dt} = 4\pi a_i^2 V_{0,i} (J_i^{gr} - J_i^{dec}) \tag{2.32}$$

where $\mathrm{V}_i = \frac{4}{3}\pi a_i^3$ is the grain volume and $\mathrm{V}_{0,i}$ is the initial volume of the nominal monomer of dust. Differentiating V_i finally

$$\frac{da_i}{dt} = V_{0,i}(J_i^{gr} - J_i^{dec}) = \left(\frac{da_i}{dt} \right)^{gr} - \left(\frac{da_i}{dt} \right)^{dec} \tag{2.33}$$

Growth rate

The growth is assumed to proceed through addition of molecules from the gas phase through suitable reactions and the growth rate for a certain species i is defined as the minimum between the rates of effective collisions on the grain surface of the gas molecules involved in the formation of the dust monomer. The species determining such rate is called "rate-determining species". With these assumptions it is possible to write

$$J_i^{gr} = \min \left[s_i \frac{\alpha_i n_{j,g} \nu_{th,j}(T_{gas})}{s_j} \right] \tag{2.34}$$

where $\mathrm{n}_{j,g}$ is the number density of the molecule j in the gas phase, s_j its stoichiometric coefficient, s_i the stoichiometric coefficient of the monomer of the dust species i, α_i its sticking coefficient, T_{gas} is the temperature of the gas given by

$$T(r)^4 = T_{eff}^4 \left[W(r) + \frac{3}{4}\tau \right] \tag{2.35}$$

where W(r) is the dilution factor and τ is the optical depth and $\nu_{th,j}(T_{gas})$ is the thermal velocity of the molecule j.

Destruction rate

In general the evaporation of a grain proceeds through pure sublimation (J_i^{sub}) due to heating by the stellar radiation but for species that can react with H_2 it can also occur a process called chemisputtering that proceeds at the grain surface through the inverse reaction of grain growth (J_i^{cs}). The total destruction rate is then

$$J_i^{dec} = J_i^{sub} + J_i^{cs} \tag{2.36}$$

Determining J_i^{sub} is immediate assuming that in chemical equilibrium it must be equal to the growth rate and it should be the same also outside equilibrium. From equation 2.34, substituting $n_{j,g}$ with the partial pressure and the temperature

$$J_i^{sub} = \alpha_i \nu_{th,i}(T_{dust}) \frac{p(T_{dust})}{k_B T_{dust}} \tag{2.37}$$

where T_{dust} is the dust equilibrium temperature and $\nu_{th,i}(T_{dust})$ is the thermal velocity of the molecules ejected from the grain surface. Using for $p(T_{dust})$, the saturated vapour pressure at the dust temperature, the Clausius-Clapeyron equation gives

$$\log p(t_{dust}) = -\frac{c_1}{T_{dust}} + c_2 \tag{2.38}$$

with c_1 containing the latent heat of sublimation of the dust species and c_2 slightly dependent on temperature.
It is possible to determine J_i^{cs} in a similar way assuming that growth and destruction rate at equilibrium must balance, using the chemical equilibrium to determine the partial equilibrium pressure of the rate-determining species, $p_{j,eq}$, obtaining

$$J_i^{cs} = s_i \frac{\alpha_i n_{j,g} \nu_{th,j}(T_{gas})}{s_j} \frac{p_{j,eq}}{k_B T_{gas}} \tag{2.39}$$

2.5 The effect of the C/O ratio

As mentioned in the previous chapters, the surface chemistry of an AGB star depends on processes such as dredge up and hot bottom burning, that ultimately determine the ratio of carbon over oxygen. Whichever element is less abundant will be locked up in the strongly bound CO molecule while the other one will dominate the chemistry. In the case of C stars the chemistry will be rich in carbon compounds especially the very stable amorphous carbon. These are believed to be the wind drivers for this kind of stars

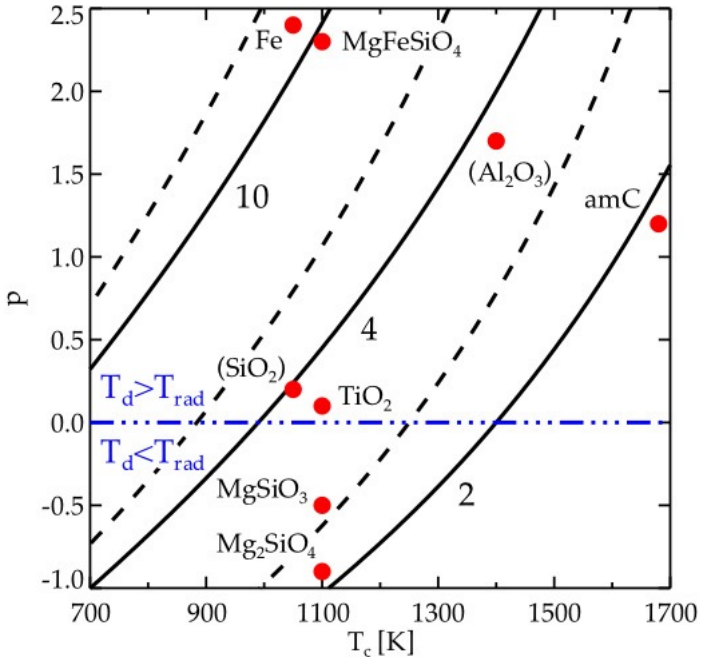

Figure 2.4: Lines of constant condensation distance as function of condensation temperature and power law coefficient and position on the p/T_c plane of different condensates. From Bladh and Höfner (2012).

thanks to their high condensation temperature, which allows them to have a small condensation distance, and their high opacity in the optical and near IR spectral region. On the other hand, M stars will be dominated by oxygen compounds, from simple oxides to more complex molecules. These are characterised by low condensation temperatures, if compared to amorphous carbon, thus are unable to condensate as close to the star. This fact highlights that driving a wind in an oxygen rich star requires a more complex mechanism than the one assumed until now.
In figure 2.4 are plotted curves of constant condensation distance as a function of the condensation temperature and the power law coefficient. The solid line corresponds to a star with $T_\star = 2800K$, the dashed one to a star with $T_\star = 2500K$. The different condensates have different positions on the p/T_c plane, marked by a red circle.

2.6 Requirements of wind drivers

To summarize the results obtained until now, the possibility of a certain condensate to be a candidate for driving the wind depends on three main

aspects:

- it should have a small condensation distance at which it is thermally stable, determined by its condensation temperature T_c and its infrared slope of the absorption coefficient p;
- there should be a sufficiently large abundance and a high degree of condensation of the limiting element of the grain material;
- it should be characterized by a high absorption or scattering efficiency of its material in the wavelength region where the stellar flux has its maximum.

Chapter 3

The problem: M-type stars

In contrast with the amorphous carbon produced in C-type stars, which is characterized by a high condensation temperature that allows it to form close to the star, the chemistry in the oxygen rich atmosphere of an M-type star cannot produce chemical species capable of driving the wind through radiation pressure alone. In its atmosphere the most stable molecule is the aluminium oxide (Al_2O_3), present as close as $1.5R_\star$ from the star, but such oxide is not abundant enough and has a low opacity. On the opposite, the abundant pure silicates like Mg_2SiO_4 are less stable and have low opacities in the relevant spectral region (around 1μm). Lastly, solid iron and Fe-Mg silicates are opaque in the relevant wavelength region but are even less stable than the pure silicates.
The following sections will get into the details of this problem and its possible solutions.

3.1 Too little radiation pressure on dust grains

Stationary models and dynamical models (with a pulsating atmosphere) that adopt grey radiative transfer show pulsation-enhanced dust-driven winds from M-type stars, but the a-posteriori frequency-dependent radiative transfer analysis with simplified dust formation finds low radiation pressure on the dust.
Woitke (2006) presents a model built in spherical symmetry that uses the piston approximation for simulating a pulsating atmosphere. It also uses a new frequency dependent Monte Carlo radiative transfer technique where dust opacities are calculated in the Rayleigh limit of the Mie theory. The dust formation rate is described by a system of differential moment equation considering grains composed of a mixture of Mg_2SiO_4, SiO_2, Al_2O_3, TiO_2 and solid Fe. The hydrostatic, dust-free solution, as can be seen from the upper panel of figure 3.1, shows a pronounced step of almost 1000K in the gas temperature structure around $1.25R_\star$ which could not be predicted by a

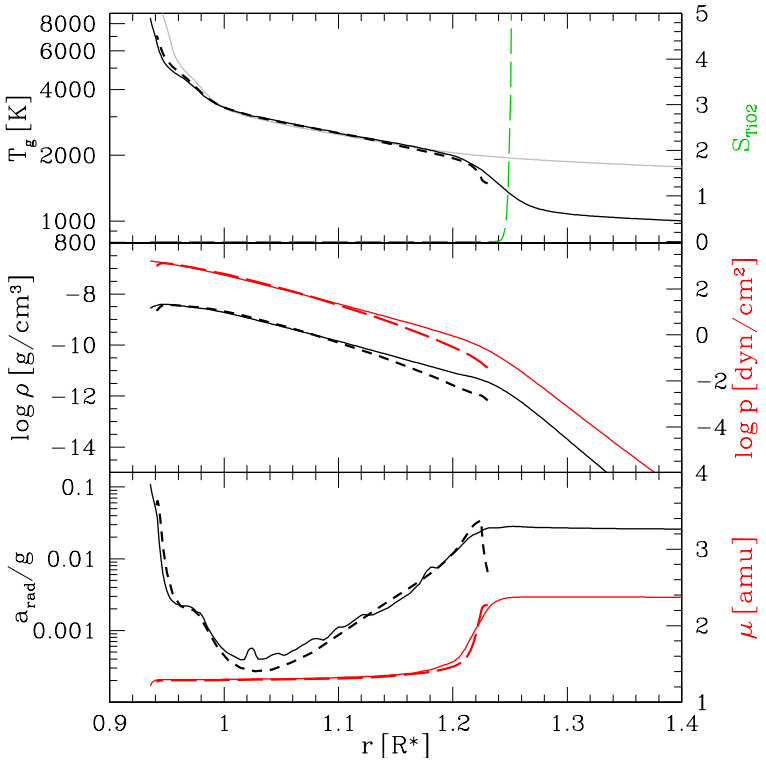

Figure 3.1: Hydrostatic initial model (solid line) in comparison to a spherical model (MARCS, dashed line) and a grey model (grey line in the first plot). On the y axis, from top to bottom, from left to right, are showed the gas temperature, the density and Γ in black, the supersaturation of TiO in green, the pressure and the mean molecular weight in red. The parameters used are $M_\star = 1 M_\odot$, $T_\star = 2800$ K, $\log g = -0.6$, $L_\star = 6048 L_\odot$, $Z = 1$. From Woitke (2006).

grey model (marked by the grey line in the same panel), but is very important because the lower temperatures allow the formation of dust.

Considering an optically thin dust, he calculated the maximum possible radiative acceleration by dust, with the result that he was unable to drive the wind, as is evident looking at the lower panel of figure 3.1 that shows the value of the ratio between radiative acceleration and gravity. Even in the region beyond $1.2 R_\star$ its value is smaller than unity.

This can be explained by the fact that the dust temperatures and opacities are strongly material-dependent. The glassy character of the oxides and pure silicates, due to their low absorption coefficients in the optical and near IR spectral region, prevent their efficient heating by the star and allows them to exist very close to the star, but as a consequence they are subject to little radiation pressure and thus cannot drive a wind, as can be seen in table 3.1.

solid material	$\frac{\rho_{dust}}{\rho_{gas}}[10^{-3}]$	$1.5R_\star$	$2R_\star$	$5R_\star$
TiO_2	0.0061	1030 K	750 K	380 K
		0.00004	0.00004	0.00005
Al_2O_3	0.11	1090 K	810 K	420 K
		0.0013	0.0014	0.0015
SiO_2	1.6	1000 K	740 K	380 K
		0.032	0.034	0.036
Mg_2SiO_4	1.9	1150 K	850 K	430 K
		0.022	0.024	0.025
$MgFeSiO_4$	4.0	1930 K(u)	1710 K(u)	**1170 K**
		1.3	1.4	**1.4**
$MgSiO_3$	2.3	1010 K	740 K	380 K
		0.025	0.027	0.029
$Mg_{0.5}Fe_{0.5}SiO_3$	3.0	1880 K(u)	1580 K(u)	690 K
		0.21	0.21	0.18
Fe	1.3	1980 K(u)	1770 K(u)	1280 K
		0.85	0.89	0.88
am. carbon	3.0	1870 K(u)	**1640 K**	**1130 K**
C/O = 1.5		20	**21**	**21**

Table 3.1: Dust temperatures and dust radiative acceleration in the case of full condensation into small particles in the static model. Temperatures followed by (u) mark thermally unstable condensates. The rows immediately under the dust temperatures show Γ for each condensate. From Woitke (2006).

The dust temperatures and Γ values for silicates, solid iron and iron-rich silicates obtained from the model are showed in table 3.1. Pure silicates have low Γ values: their condensation is without effect in driving the wind. Solid iron has Γ close to one but is unstable. Finally, iron-rich silicates have high Γ values but are unstable and condense at large radii, where the density is low and the radiative acceleration is inefficient. The mass loss rates obtained from this model were lower than $10^{-10}M_\odot/yr$ and even approaching extreme stellar parameters led to almost the same conclusion.

To see what the wind could look like he artificially enhanced the radiative acceleration by setting $\Gamma = \Gamma_{gas} + 5\Gamma_{dust}$. The resulting model showed warm molecular layers (predicted also by normal models) truncated by the "step" in the gas temperature, with the pulsation of the star that led to a time-dependent extension of these layers to up to two stellar radii. The formation of seed particles happened just above these layers, where the gas was cold ($700K - 900K$) and sufficiently dense. The model developed two

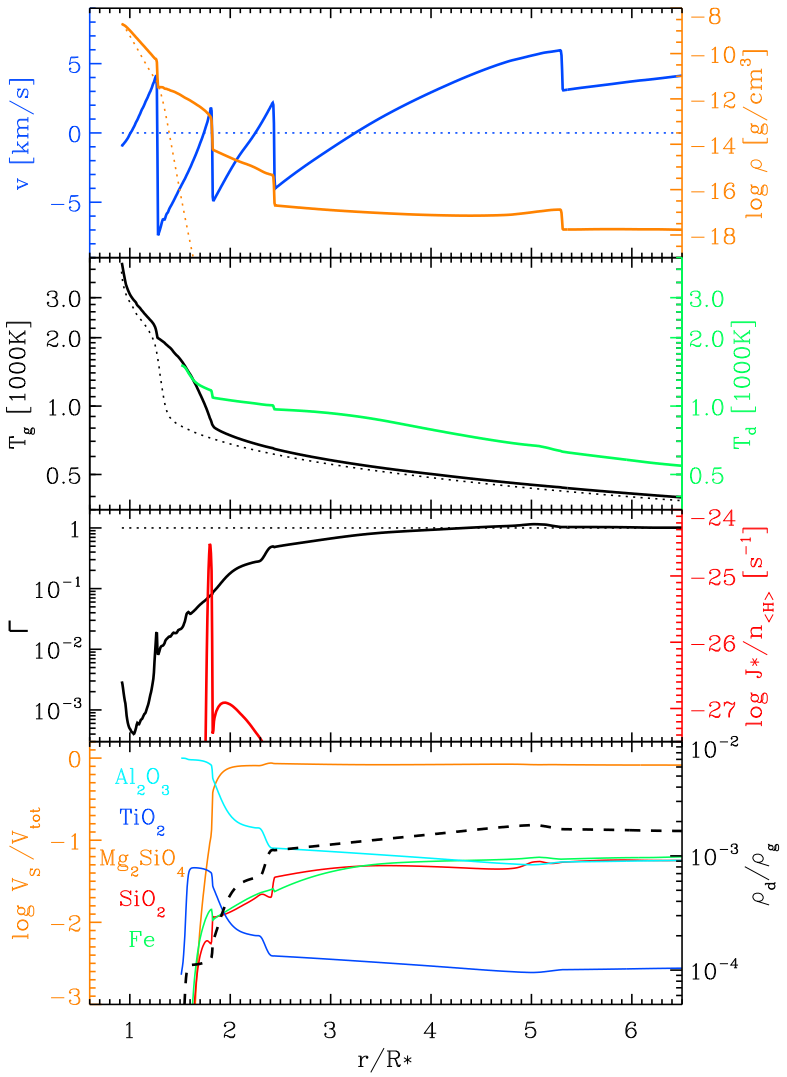

Figure 3.2: Dynamical wind model after 100 years of simulation time with an enhanced Γ. First panel: velocity (blue) and density (orange). Second panel: gas temperature (black) and dust temperature (green). Third panel: Γ (black) and nucleation rate (red). Fourth panel: volume fraction of solid material s (different colour foe each compound) and ratio between dust density and gas density (orange).The parameters used were: $M_\star = 1 M_\odot$, $T_\star = 2500$ K, $L_\star = 10000 L_\odot$, $Z = 1$, piston period $P = 600$ days, velocity amplitude $\Delta v = 2$ km s^{-1}, enhanced Γ. From Woitke (2006).

different dust layers. The closest to the star was at a distance larger than $1.5R_\star$ and at a temperature lower than $1500K$ and was composed of pure Al_2O_3. Further out, on top of the Al_2O_3 particles, formed the more opaque Mg-Fe silicates. The dynamical model after 100 years of evolution is showed in 3.2.
Woitke (2006) also determined that the temperature of the grains is strongly dependent on its iron content. The volume fraction of solid iron inclusions in the grains is determined by the fact that its increase would cause too much radiative heating and a subsequent re-evaporation of the inclusions[1]. The iron content then adapts rapidly to any changes in the ambient medium unless the density becomes too small: the degree of condensation of Fe reached a low final value of about 17% in the model.
With these conditions, the radial acceleration exceeds the gravitational deceleration only beyond $3.5 - 4R_\star$ and as a consequence the mass loss rate is low ($\dot{M} \approx 2.3 \times 10^{-9} M_\odot/yr$) as well as the terminal velocity ($\langle v_\infty \rangle \approx$ 2.6 km s^{-1}).

3.2 Micrometer-sized dust grains as wind drivers

A possible solution for driving the winds in M-type stars is given by Höfner (2008) and is studied by Bladh and Höfner (2012), Bladh (2014), Bladh, Höfner, et al. (2015).
As the starting point, they assume that a certain grain can be a wind driver if it has a sufficiently high mean flux opacity per mass and if it can form in the particular atmosphere of AGB stars in sufficient quantities.
An alternative way to express the first condition is writing

$$k_H > k_{crit} = \frac{4\pi c G M_\star}{L_\star} \tag{3.1}$$

where k_H is the flux mean opacity, while the second one can be divided in two different requirements: the grains should be able to form close to the star, thus should have a small condensation distance, and should grow fast enough within the given physical and chemical conditions, thus requiring a certain abundance of its raw elements and a higher density. As previously outlined, molecules such as olivine ($Mg_{2x}Fe_{x(2-1)}SiO_4$) or pyroxene ($Mg_xFe_{1-x}SiO_3$) are the most abundant dust species in M-type AGB stars, thus are candidates for driving a wind.
Using equation 2.26 it is possible to estimate the condensation distance of the different kinds of condensates that can form in the oxygen-rich atmosphere with the assumption that $T_\star \sim 3000K$. For a silicate grain with iron

[1]It is useful to remember that Fe has p=1: from eq. 2.26 it is immediate that it will heat very much when exposed to the radiation field of the star.

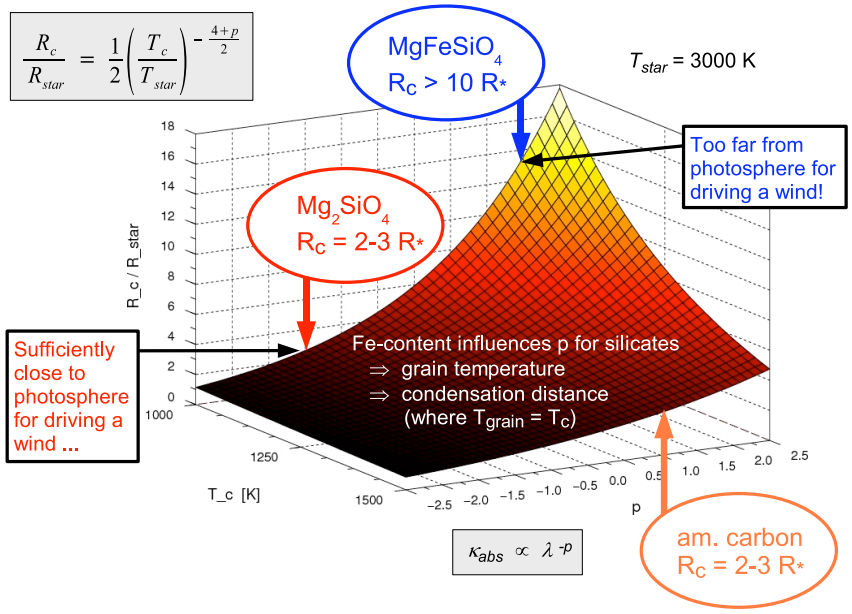

Figure 3.3: Condensation distance as a function of the power law index of the absorption coefficient p for a range of condensation temperatures, assuming $T_c = 3000$ K. The positions on the p/T_c plane of the most important grain types are indicated. From Höfner (2011).

inclusions p becomes of the order of 2 and assuming $T_c \sim 1000K$ if follows that $\frac{R_c}{R_\star} > 10$. On the other hand iron-free silicates have p∼-1 thus $\frac{R_c}{R_\star} \approx 2-3$, which makes them the perfect candidates for driving the wind. These facts also explain once more why silicate grains must be iron-free to be able to drive the wind. Figure 3.3 gives a visualization of these results.
Still, the problem of the low opacity of the candidates in the relevant spectral region remains, resulting in a low absorption cross section and a negligible radiative acceleration.

3.2.1 Scattering by large dust grains

Starting from equation 2.16 it is possible to determine the contribute of a certain dust grain to driving a wind weighting the total opacity with the relative flux, obtaining the monochromatic flux-weighted opacity

$$\tilde{k}_{acc}(\lambda, a_{gr}, T_\star) = k_{acc}(\lambda, a_{gr}) \frac{\lambda B_\lambda(T_\star)}{T_\star^4 \frac{\sigma}{\pi}} \tag{3.2}$$

that must be larger than k_{crit} for wind driving species. The black contour in figure 3.4 shows the region where the opacity of forsterite exceeds the critical

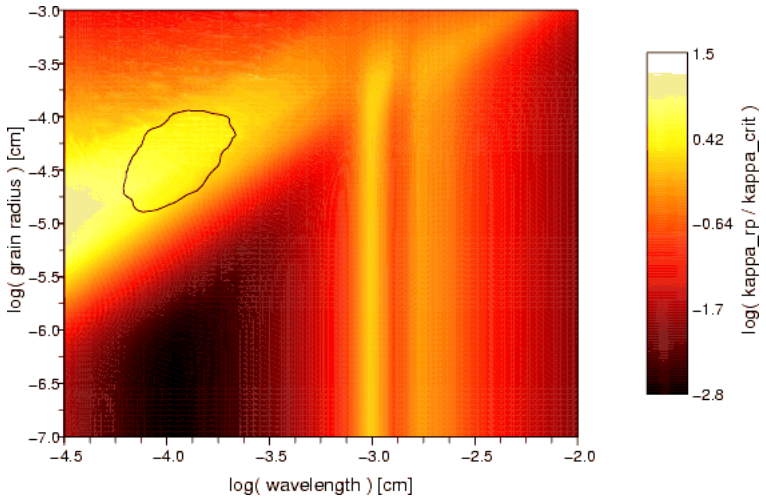

Figure 3.4: Opacity of forsterite grains in unit of the critical opacity assuming $M_\star = 1M_\odot$, $L_\star = 7000L_\odot$ and 30% of Si condensed intro grains. The region inside the black contour marks where the flux-weighted opacity exceeds the critical opacity, assuming a Planckian flux distribution with $T_\star = 2700$ K. From Höfner (2008).

value.
From this requirement, Höfner (2008) derives that the size of the grains must be in a narrow interval around $0.3\mu m$ (from $0.1\mu m$ to $1\mu m$) for the grain species to be able to drive the wind. In these conditions the previous assumption of small particle limit (compared to the wavelength) breaks. Particles with dimensions in the micrometer range have high radiative scattering cross section that can become larger than the radiative absorption cross section, thus overcoming the problem of the low absorption cross section and resulting in a sufficient radiative acceleration to drive a wind. This hypothesis is then explored by Bladh and Höfner (2012) and Bladh, Höfner, et al. (2015) with the result that scattering on large dust grains could drive the wind, especially micron-sized Mg_2SiO_4 grains due to the abundance of its elements and to its small condensation distance.

3.3 A complementary perspective

Nanni et al. (2013) offers an interesting hint that may be relevant in view of solving the problem in M-type stars.
Analysing the experimental results by Nagahara & Ozawa (1996) it is possible to determine that the destruction rate of forsterite in presence of hydrogen molecules (chemisputtering) grows linearly with the gas pressure and Gail & Sedlmayr (1999) concluded that this process should be very efficient within

the circumstellar envelopes (CSEs) of AGB stars resulting in $J_i^{sub} \ll J_I^{cs}$ so that $J_i^{dec} \approx J_I^{cs}$. For species which do not react with hydrogen $J_i^{dec} = J_I^{sub}$. However, the efficiency of chemisputtering is still a matter of debate. On the theoretical side it is supposed that it could be inhibited by the high activation energy barrier of the reduction reaction of silicate dust compounds by H_2. On the observational side there is evidence from experiments that the condensation temperature of crystalline forsterite (iron-free olivine) and crystalline enstatite (iron-free pyroxene) at pressures corresponding to stellar winds is between 1400K and 1500K. These condensation temperatures are significantly higher than the ones predicted by models that adopt a fully efficient chemisputtering. These results are not in contradiction with the results of Nagahara & Ozawa (1996) because they found evidences for chemisputtering at a gas pressure considerably higher than the one at which the dust is supposed to form in the CSEs. Nanni et al. (2013) then computed a class of models without chemisputtering, where the evolution of the grain is given by eq. 2.33 with

$$J_i^{dec} = J_i^{sub} \tag{3.3}$$

In their model the sublimation rate depends on the dust equilibrium temperature which in turn can be defined only near the condensation point. Instead of integrating eq. 2.33 they determine the condensation point within the CSE by comparing the growth rate with the maximum sublimation rate obtained setting $\alpha_i = 1$ in eq. 2.37, also defined by $J_i^{gr} = J_{i,max}^{dec}$ thus allowing to determine the condensation temperature. Beyond this point the grain grows with the assumption that the sublimation rate is negligible. The condensation temperature then depends on one side on the dust species which determine $J_{i,max}^{dec}$ and on the other side on the physical conditions of the CSE, which determine J_i^{gr}. The real sublimation rate, however, is only α_i times the maximum sublimation rate so the condensation begins when

$$J_i^{gr} = \frac{1}{\alpha_i} J_{i,max}^{sub} \tag{3.4}$$

and the corresponding super-saturation ratio behaves similarly. The accuracy of the results is not affected by the assumption of negligible sublimation rate because beyond the condensation point J_i^{sub} decreases almost exponentially with the temperature.

An estimate of the condensation temperature of silicates as a function of $(\frac{da_i}{dt})^{gr}$ is shown in figure 3.5. The solid and the dotted line refer to the case of olivine and pyroxene with J_i^{sub} from Kimura et. al. (2002). The evaporation of pyroxene is supposed to occur preferentially through SiO_2 molecules (empirically $c_1 = 6.99 \times 10^4$, $\exp(c_2) = 3.13 \times 10^{11}$dyne cm^{-2}) and from eq. 2.38 the resulting condensation temperatures lie between 1400K and 2000K. In the case of olivine ($c_1 = 6.56 \times 10^4$, $\exp(c_2) = 6.72 \times 10^{14}$dyne cm^{-2}) they are instead between 1200K and 1400K. The resulting condensation temperatures are considerably higher than those found in presence of efficient

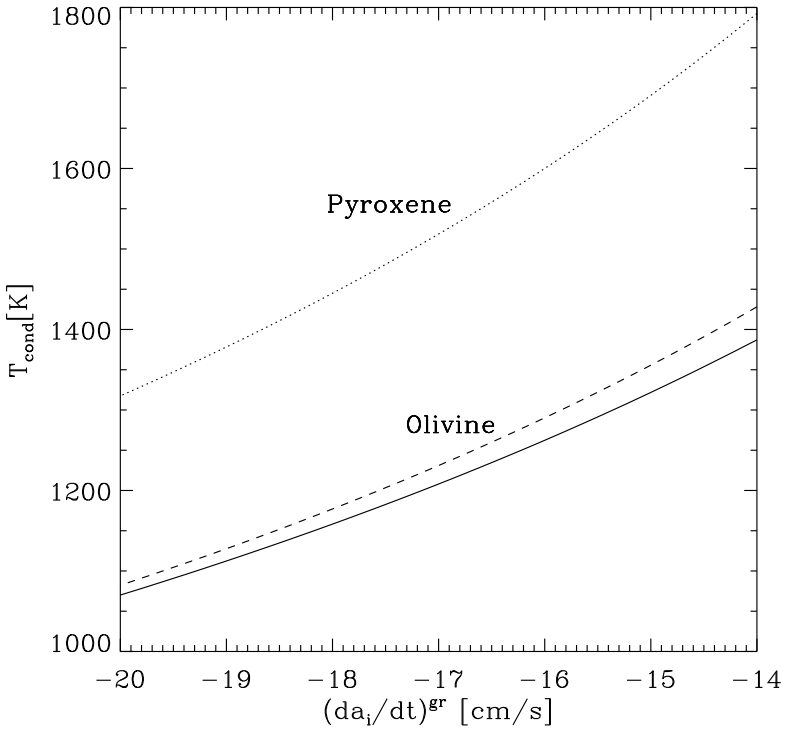

Figure 3.5: Condensation temperatures of olivine and pyroxene as a function of the growth rate assuming $J_i^{dec} = 0$. From Nanni et al. (2013).

chemisputtering. Finally, the dashed line is obtained through the analytical fits to theoretical calculations of c_1 and c_2, provided by Duschl et al. (1996) and shows comparable results.
The results obtained in the case of olivine are in good agreement with recent experiments by Nagahara et al. (2009a) that found condensation temperatures between 1350K and 1450K. Instead, in the case of pyroxene the results are very different. A possible reason is that the evaporation of pyroxene is assumed to occur through SiO_2 molecules but it is not considered that this process is followed by the formation of forsterite, which immediately evaporates at these temperatures. Nanni et al. (2013) consider the results for pyroxene as an upper limit while the results for olivine as representative of all silicates.

Bibliography

Bladh, S. (2014). "Dynamical atmospheres and winds of M-type AGB stars". thesis. Department of Physics and Astronomy of Uppsala University.

Bladh, S. and S. Höfner (2012). "Exploring wind-driving dust species in cool luminous giants. I. Basic criteria and dynamical models of M-type AGB stars". In: *Astronomy & Astrophysics, Vol. 546.*

Bladh, S., S. Höfner, et al. (2015). "Exploring wind-driving dust species in cool luminous giants. III. Wind models for M-type AGB stars: dynamic and photometric properties". In: *Astronomy & Astrophysics, Vol. 575.*

Habing, Harm J. and Hans Olofsson (2004). *Asymptotic Giant Branch Stars.*

Höfner, S. (2008). "Winds of M-type AGB stars driven by micron-sized grains". In: *Astronomy & Astrophysics, Vol. 491.*

— (2009). "Dust Formation and Winds around Evolved Stars: The Good, the Bad and the Ugly Cases". In: *Cosmic Dust - Near and Far ASP Conference Series, Vol. 414.*

— (2011). "Starlight and Sandstorms: Mass Loss Mechanisms on the AGB". In: *Why Galaxies Care about AGB Stars II: Shining Examples and Common Inhabitants - ASP Conference Series, Vol. 445.*

— (2015). "Wind Acceleration in AGB Stars: Solid Ground and Loose Ends". In: *Why Galaxies Care about AGB Stars III: A Closer Look in Space and Time - ASP Conference Series, Vol. 497.*

Lamers, Henny J. G. L. M. and JosephP. Cassinelli (1999). *Introduction to Stellar Winds.*

Nanni, Ambra et al. (2013). "Evolution of thermally pulsing asymptotic giant branch stars - II. Dust production at varying metallicity". In: *Monthly Notices of the Royal Astronomical Society, Volume 434, Issue 3.*

Sedlmayr, Erwin and Jan Martin Winters (1997). "Cool Star Winds and Mass Loss: Theory". In: *Stellar Atmospheres: Theory and Observations.*

Willson, Lee Anne (2000). "Mass Loss From Cool Stars: Impact on the Evolution of Stars and Stellar Populations". In: *Annual Review of Astronomy and Astrophysics, Vol. 38.*

Woitke, P. (2006). "Too little radiation pressure on dust in the winds of oxygen-rich AGB stars". In: *Astronomy & Astrophysics, Vol. 460.*